Self-Assembly of Daisy Chain Oligomers from Heteroditopic Molecules Containing Secondary Ammonium Ion and Crown Ether Moieties

HARRY W. GIBSON,[1] NORI YAMAGUCHI,[1]* ZHENBIN NIU,[1] JASON W. JONES,[1]† CARLA SLEBODNICK,[1] ARNOLD L. RHEINGOLD,[2]‡ LEV N. ZAKHAROV[2]§

[1]Department of Chemistry, Virginia Polytechnic Institute and State University, Blacksburg, Virginia 24061

[2]Department of Chemistry, University of Delaware, Newark, Delaware 19716

Received 28 September 2009; accepted 1 December 2009
DOI: 10.1002/pola.23861
Published online in Wiley InterScience (www.interscience.wiley.com).

ABSTRACT: MALDI-TOF MS of the heteroditopic compound **2**-(benzylammoniomethyl)dibenzo-24-crown-8 hexafluorophosphate (**4**) revealed oligomeric "daisy chain" species up to the hexamer. Similar results were obtained for 2-(6′-hydroxyhexylammoniomethyl)dibenzo-24-crown-8 hexafluorophosphate (**8**). The complexations of two substituted dibenzylammonium salts, 2,2′-dimethyldibenzylammonium hexaflurophosphate (**9a**) and 2,2′,5-trimethoxydibenzylammonium hexafluorophosphate (**9b**), with dibenzo-24-crown-8 were examined as models for slippage systems; association constants are reported for these systems. A crystal structure is reported for the new dimethylbenzylammonoium pseudorotaxane. The trimethoxy analog is shown to be capable of slippage formation of a rotaxane, albeit in low yield. © 2010 Wiley Periodicals, Inc. J Polym Sci Part A: Polym Chem 48: 975–985, 2010

KEYWORDS: crown ether; crystal structure; host–guest systems; macrocycles; mass spectrometry; pseudorotaxane; self-organization; supramolecular polymer

INTRODUCTION

Pseudorotaxanes and rotaxanes[1] now are strong contributors to the realm of supramolecular science.[2] These molecular recognition motifs have been applied to the self-assembly of an ever increasing variety of architectures such as dendrimers[1,3] and polymeric systems.[1,4] Efforts continue toward the spontaneous construction of ordered linear pseudorotaxane arrays,[1,5] so called "daisy chains," a subclass of supramolecular polymers.[6] One approach is to use complementary pairs of homoditopic molecules[5(c,d)]; another is to use heteroditopic molecules.[5(a,b,d,e)] Scheme 1 illustrates the general approach to create such linear arrays **2** from heteroditopic molecules **1**. The use of a single building block of this type is advantageous because it guarantees the 1:1 stoichiometry between the complementary units required for effective formation of supramolecular aggregates in an essentially step growth process.

Some years ago,[7] we pursued this methodology using the complementary dibenzo-24-crown-8 (DB24C8)/dibenzylammonium pair, specifically **4**. Then Stoddart and his coworkers reported the isolation and X-ray structure of the cyclic dimeric pseudorotaxane complex **3**, $n = 2$ from the trifluoroacetate analog of **4** (Scheme 1).[5(a)] This coupled with the solubility considerations noted later led to our essential abandonment of this project. Subsequently, Stoddart et al. reported their extensive studies of this system and several analogs.[5(d)] Our efforts also explored another avenue for enhancing both the solubility and self-association in analogous heteroditopic systems and examined potential slippage-based approaches to their rotaxane analogs; here, we summarize those studies.

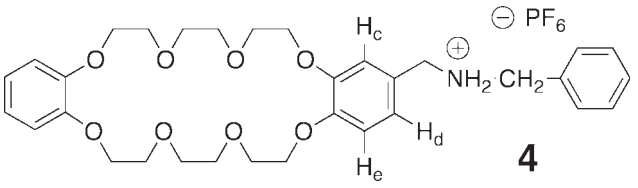

4

RESULTS AND DISCUSSION

Daisy Chain Polymers

The synthesis of heteroditopic (A-B) monomer **4** is outlined in Scheme 2. Aldehyde **5** was prepared from the previously reported alcohol[5(c)] by PCC oxidation and converted to the

Additional Supporting Information may be found in the online version of this article.
*Present address: General Electric Advanced Materials, Strongsville, Ohio 44149, USA.
†Present address: E.I. du Pont de Nemours and Company, Jackson Laboratory, Deepwater, New Jersey 08023, USA.
‡Present address: Department of Chemistry and Biochemistry, University of California, San Diego, California 92023, USA.
§Present address: Department of Chemistry and Materials Science Institute, University of Oregon, Eugene, Oregon 97403-1253.
Correspondence to: H. W. Gibson (E-mail: hwgibson@vt.edu)
Journal of Polymer Science: Part A: Polymer Chemistry, Vol. 48, 975–985 (2010) © 2010 Wiley Periodicals, Inc.

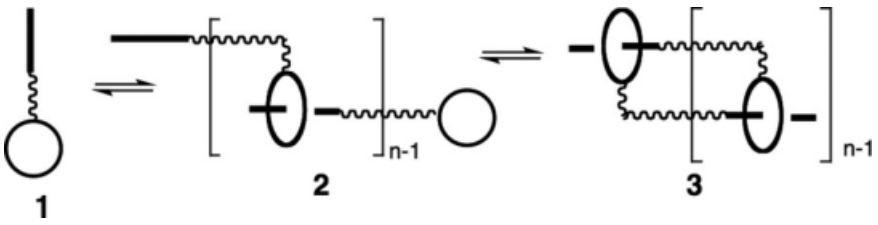

SCHEME 1 Cartoon representations of the formation of linear daisy chain arrays **2** and cyclic daisy chain species **3** by self-assembly of heteroditopic **1**. The circles and ellipses represent the DB4C8 moiety and the filled rectangles represent the dibenzylammonium moiety.

corresponding Schiff base **6a** by condensation with benzylamine. Reduction of **6a** ($NaBH_4$) produced the secondary amine **7a**, which was converted to **4** by sequential treatment with HCl and NH_4PF_6. The structure of **4** was confirmed by high-resolution mass spectrometry and its ^1H NMR spectrum in DMSO-d_6, which as a highly competitive H-bond acceptor essentially prevents pseudorotaxane formation.[5(d),8] This heteroditopic compound is essentially insoluble in halogenated solvents such as chloroform and methylene chloride; the solubility of **4** was < 50 mM in acetone and acetonitrile.

Stoddart et al. used CD_3CN as solvent and indicated that two stereoisomeric cyclic dimeric species were observed, based on signals for H_e at 6.41 ppm and H_c at 6.17 ppm in a ratio of 5:1 in 20 mM solution at 0 °C, but surprisingly claimed that no uncomplexed **4** was detected.[5(d)] Because of the complexity of the spectra, they proceeded to study various deuterated and fluorinated analogs; when the unsubstituted benzo ring of **4** was deuterated, the resulting simplified spectrum clearly revealed the two isomeric (*meso* and *racemic*, Scheme 3) cyclic dimers as separate signals for H_c (doublets, $J = 1.5$ Hz, major @ 6.78, minor @ 6.17 ppm), H_d (doublets of doublets, $J = 1.5$, 8 Hz, major @ 6.84, minor @ 6.98 ppm), and H_e (doublets, $J = 8$ Hz, major @ 6.41, minor @ 6.89 ppm); these observations confirmed the assignments made for **4** itself. These conclusions were corroborated in later work; a rotaxane containing similar units revealed the same chemical shifts.[9] Our spectra of **4** in CD_3CN were essentially identical to those reported by Stoddart et al.

The MALDI-TOF mass spectrum (MS) of a solid sample prepared by slow evaporation of a chloroform/acetonitrile (1/1 v/v) solution of **4** revealed the base peak at $m/z = 1137$ g/mol, indicating dimeric supermolecules (probably mostly the cyclic dimer) after loss of one PF_6 moiety and one HPF_6. A peak of nearly 100% intensity at $m/z = 1017$ g/mol corresponds to dimer after loss of a benzylamine fragment, one PF_6 moiety and one HPF_6. These results agree with the LSI MS results reported by Stoddart et al.,[5(d)] who detected only the dimer.

However, in our positive ion MALDI-TOF spectra,[10] there was also clear evidence of oligomeric aggregates up to the hexamer (Fig. 1, Table 1). Although these signals were weak, on the order of 0.2–4.3% of the base peak, their presence indicates that even in the polar, competitive H-bonding matrix used (dihydroxybenzoic acid) there is an equilibrium involving species larger than the dimer, probably of linear architecture. Moreover, MS obtained via FAB also revealed oligomers up to the pentamer[8] (Table 1).

Some years ago Busch et al. proposed and demonstrated that incorporation of suitable hydrogen bonding terminal moieties could enhance formation of pseudorotaxane complexes.[11] Utilizing this concept to enhance solubility and augment the threading process and additionally provide a route to rotaxane systems via reactions on the hydroxyl group, we prepared the 6-hydroxyhexyl analog, **8** (Scheme 2). The spectrum of **8** in CD_3SOCD_3 (Fig. 2) is similar to that of **4** in the same solvent in the aromatic and ethyleneoxy regions, but contains additional signals for the hydroxyhexyl unit. Solutions of **8** in CD_3COCD_3 were also examined by ^1H NMR spectroscopy;[12]

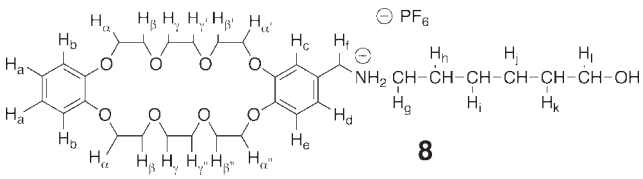

as can be seen in Figure 3 these spectra are complicated. The signals assigned to H_e and H_c are observed as a doublet and a broad singlet at 6.65 and 6.33, respectively, both ~0.2 ppm upfield from the signals observed by Stoddart et al. for the cyclic dimer of **4** in CD_3CN.[5(d)] Interestingly, the ratio of these

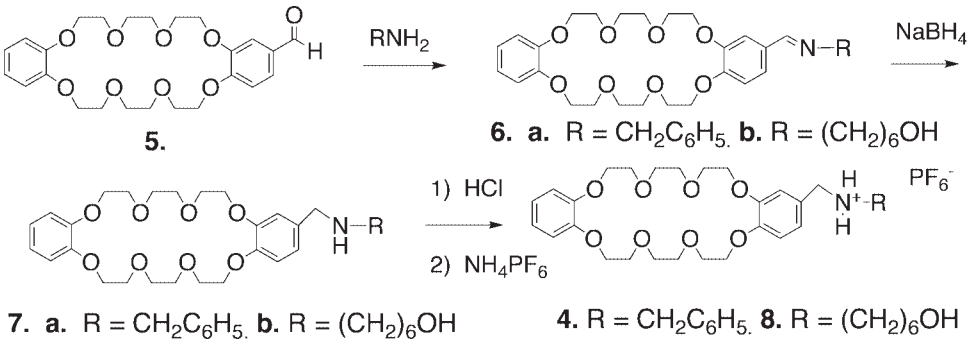

SCHEME 2 Synthesis of heteroditopic 2-alkylammoniodibenzo-24-crown-8 hexafluorophosphates **4** and **8**.

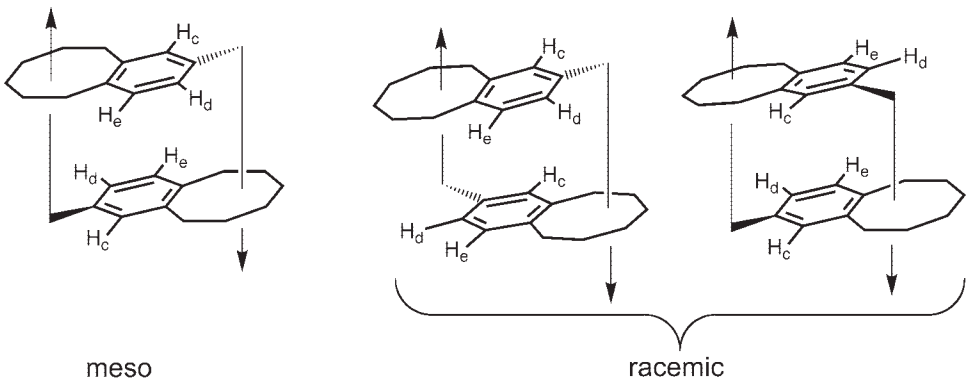

SCHEME 3 Representations of the *meso* and D,L-diasteromers of the cyclic dimer from **4**.

peaks, assumed to be the major H_e and minor H_c, was constant at 13 across the concentration range from 0.60 to 10 mM. Assuming these signals correspond to the major and minor isomers of the cyclic dimer as assigned by Stoddart et al.,[5(d)] inasmuch as the equilibrium between the cyclic dimers is not concentration dependent, the higher ratio relative to that in **4** indicates that formation of the cyclic dimer is more selective in this case, perhaps as a consequence of the greater steric constraints imposed by the hydroxyhexyl group, but affords the same predominant diastereomer (perhaps the racemate, Scheme 3[5(d)]) as **4** in CD_3CN. Note that the proportions of these signals relative to the rest of the aromatic region did not change, again as in the case of **4**[5(d)] very surprisingly suggesting that the cyclic dimer concentration is essentially constant. However, other changes are observed: the signal at 3.75 ppm is drastically reduced in intensity as the concentration increases, while concomitantly the signal at ~4.5 ppm also changes. Indeed, these observations mirror those for **4**. Unfortunately, we are unable to analyze these spectra in quantitative fashion.

However, both MALDI-TOF (Fig. 4) and FAB[8] MS of **8** (Table 2) provide clear evidence of self-assembly into dimeric, trimeric, tetrameric, and pentameric aggregates even in very polar, competitively hydrogen bonding matrices.

A feature of this particular system that has not been recognized previously is its tacticity. Just as the diastereomeric relationships between adjacent repeat units in polystyrene or polypropylene lead to isotacticity and syndiotacticity, the present systems also give rise to tacticity as illustrated in Scheme 4. It may be that tacticity in the oligomeric daisy chains produces the same level of diastereoselectivity as observed with the cyclic dimers. It is also possible that the chemical shifts of protons H_c, H_d, and H_e are the same in the linear and cyclic species. Moreover, the equilibrium between linear and cyclic species could be rapid relative to the NMR time scale, resulting in time-averaged signals for these protons. If this is true, it explains the otherwise puzzling fact that the proportion of major and minor signals is independent of concentration.

Slippage Studies

Examination of CPK molecular models reveals that the phenyl groups at the termini of dibenzylammonium salts are relatively bulky compared to the cavity size of DB24C8. We were therefore curious about the effect of substituents purposely placed on the phenyl rings of dibenzylammonium salts on the formation of pseudorotaxanes. As models for slippage[1,13] systems dialkylammonium salts **9a** and **9b** were

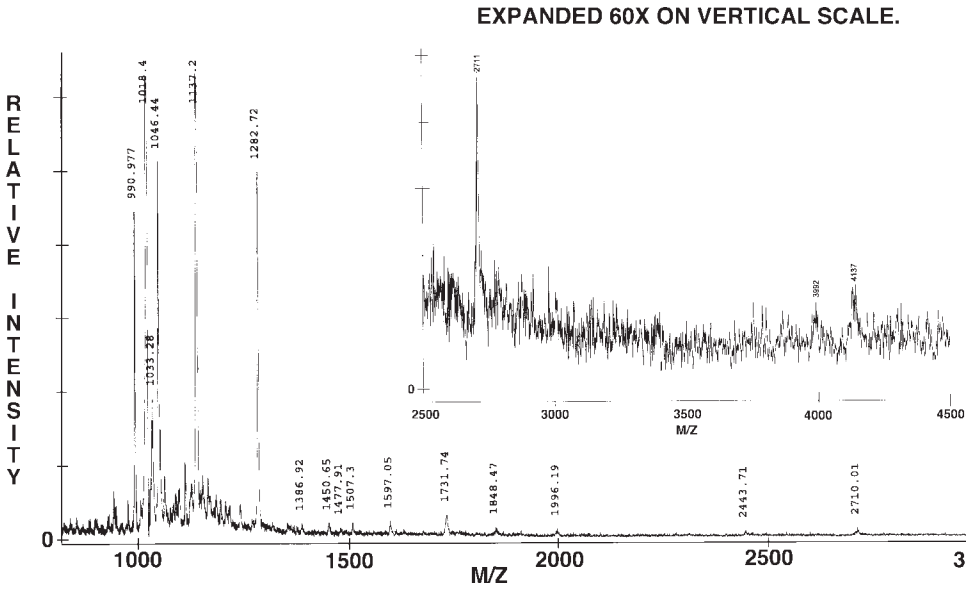

FIGURE 1 The MALDI-TOF mass spectrum of a solid sample prepared from **4** in dihydroxybenzoic acid matrix, showing self-assembled oligomers. See Table 1 for assignments and details.

TABLE 1 Supramolecular Formulae, Calculated Supramolecular Exact Masses, and Observed (MS) Mass/Charge Ratios from M = **4**·PF_6

Structure	Supramolecular Formula	Calcd.	Obs (*m/z*)	Intensity (%)
M-HPF_6+Na	$C_{32}H_{42}NO_8Na$	590.7	590.6[a]	34
M_2-2PF_6-$C_6H_5CH_2NHCH_2$	$C_{56}H_{74}NO_{16}$	1,016.5	1,016.6[a]	99
M_2-2PF_6-$C_6H_5CH_2$	$C_{57}H_{77}N_2O_{16}$	1,045.5	1,046.4[a]	79
M_2-2PF_6	$C_{64}H_{84}N_2O_{16}$	1,137.4	1,136.7[a]	100
M_2-2PF_6	$C_{64}H_{84}N_2O_{16}$	1,137.4	1,136[b]	100
M_2-PF_6+H	$C_{64}H_{85}N_2O_{16}PF_6$	1,283.3	1,282.7[a]	79
M_2-PF_6+H	$C_{64}H_{85}N_2O_{16}PF_6$	1,283.3	1,282[b]	19
M_2+Na	$C_{64}H_{84}N_2O_{16}P_2F_{12}Na$	1,450.3	1,450.6[a]	2.6
M_3-3PF_6-$C_6H_5CH_2NHCH_2C_6H_5$	$C_{82}H_{111}N_2O_{24}$	1,507.8	1,507.3[a]	2.6
M_3-3HPF_6-$C_6H_5CH_2N$	$C_{89}H_{116}N_2O_{24}$	1,596.8	1,597.0[a]	3.0
M_3-3HPF_6-$C_6H_5CH_2N$	$C_{89}H_{116}N_2O_{24}$	1,596.8	1,598[b]	1.1
M_3-2PF_6-$C_6H_5CH_2NHCH_2$	$C_{88}H_{116}N_2O_{24}PF_6$	1,729.8	1,731.7[a]	4.3
M_3-PF_6-HPF_6	$C_{96}H_{125}N_3O_{24}PF_6$	1,848.9	1,848.5[a]	1.7
M_3-PF_6-HPF_6	$C_{96}H_{125}N_3O_{24}PF_6$	1,848.9	1,849[b]	0.68
M_3-PF_6	$C_{96}H_{126}N_3O_{24}P_2F_{12}$	1,996.0	1,996.2[a]	1.7
M_3-PF_6	$C_{96}H_{126}N_3O_{24}P_2F_{12}$	1,996.0	1,996[b]	0.35
M_4-2PF_6-$C_6H_5CH_2NHCH_2$	$C_{120}H_{158}N_3O_{32}P_2F_{12}$	2,443.0	2,443.7[a]	1.7
M_4-PF_6	$C_{128}H_{168}N_4O_{32}P_3F_{18}$	2,709.6	2,710.0[a]	1.1
M_5	$C_{160}H_{210}N_5O_{40}P_5F_{30}$	3,568.2	3,564[b]	1.9
M_6-2PF_6	$C_{192}H_{252}N_6O_{48}P_4F_{24}$	3,992.0	3,992[a]	0.20
M_6-PF_6	$C_{192}H_{252}N_6O_{48}P_5F_{30}$	4,136.9	4,137[a]	0.27

[a] MALDI-TOF mass spectrum recorded in the positive ion mode in dihydroxybenzoic acid matrix; sample prepared by evaporation of a chloroform/acetone (1/1 v/v) solution.

[b] FAB mass spectrum recorded in positive ion mode in nitrobenzyl alcohol; sample prepared by evaporation of a chloroform/acetone (1/1 v/v) solution.

prepared as shown in Scheme 5. Salt **9a** is sparingly soluble in $CHCl_3$ and CH_2Cl_2; in contrast, **9b** showed excellent solubility in $CHCl_3$ and CH_2Cl_2.

The ^{1}H NMR spectrum of an equimolar solution of **9a** and DB24C8 (10 mM in acetone-d_6) exhibits two sets of signals, indicating slow association and dissociation between the two components on the ^{1}H NMR time scale.[8] The signals for the benzylic protons of the corresponding pseudorotaxane

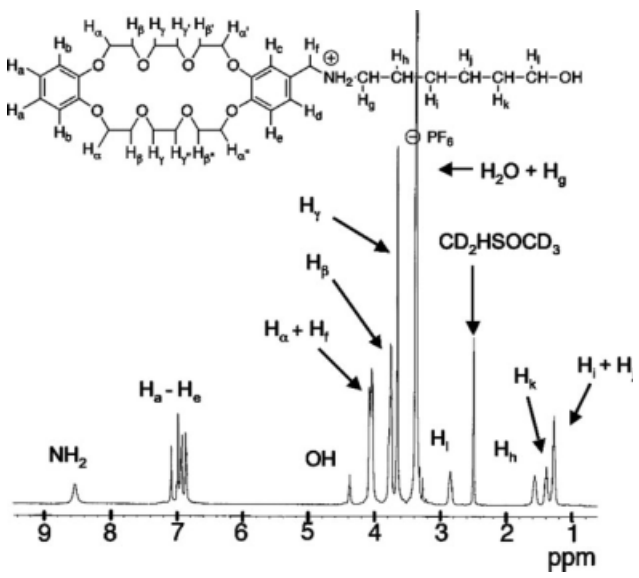

FIGURE 2 ^{1}H NMR spectrum (400 MHz, 22 °C) of heteroditopic **8** in DMSO-d_6, 20 mM.

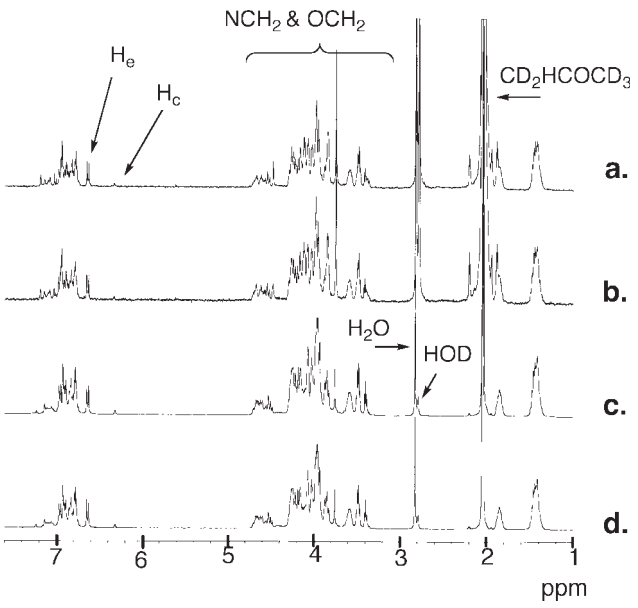

FIGURE 3 ^{1}H NMR spectra (400 MHz, 22 °C) of heteroditopic **8** in acetone-d_6: (a) 0.6 mM, (b) 1.0 mM, (c) 5.0 mM, and (d) 10 mM.

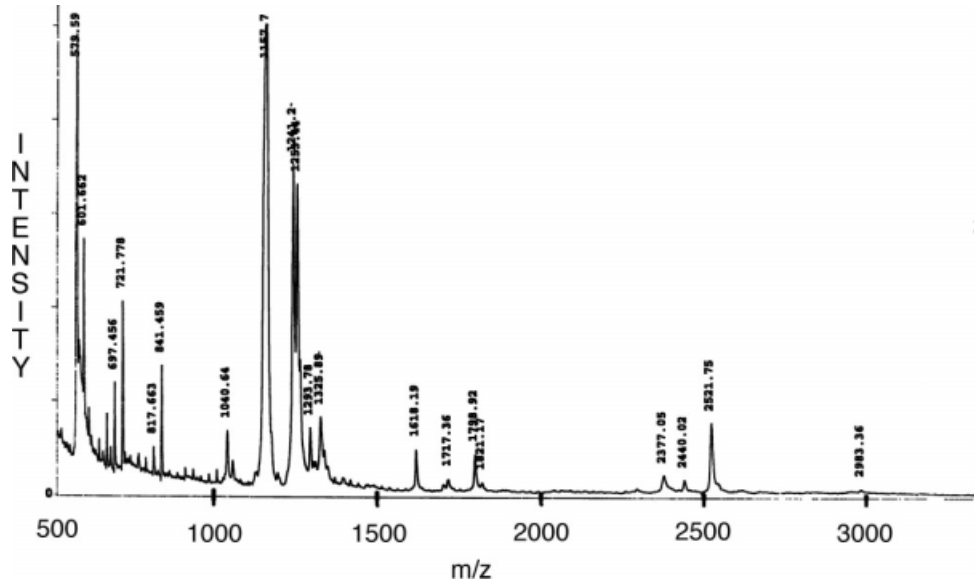

FIGURE 4 MALDI-TOF mass spectrum of a solid sample prepared from **8**, showing self-assembly of oligomers. See Table 2 for assignments and details.

exhibit significant downfield chemical shifts, indicating that they are positioned in the deshielding region of the benzo ring of the crown ether. K_{aexp} = [complex]/{[DB24C8]$_o$ − [complex]} {[**9a**]$_o$ − [complex]} = 90 M^{-1} based on the NCH_2 ^1H NMR signals.[14–16] CPK models of **9a** and DB24C8 show that a substantial force is required for the substituted phenyl ring to penetrate the cavity of DB24C8 to achieve the 1:1 pseudorotaxane geometry; the lower K_{aexp} for **9a** versus that of dibenzylammonium PF_6 (K_{aexp} = 360 M^{-1} under the same conditions[14–16]) reflects this steric constraint.

TABLE 2 Supramolecular Formulae, Calculated Supramolecular Exact Masses, and Observed (MS) Mass/Charge Ratios from M = **8**·PF_6

Structure	Supramolecular Formula	Calcd.	Obs (*m/z*)	Intensity (%)
M-PF_6+H	$C_{31}H_{49}NO_9$	579.3	579.6[a]	92
M-PF_6+Na	$C_{31}H_{48}NO_9Na$	601.3	601.7[a]	50
M-H	$C_{31}H_{47}NO_9PF_6$	722.3	721.8[a]	38
M_1+$NH_2(CH_2)_6OH$+H	$C_{37}H_{63}N_2O_{10}PF_6$	841.4	841.5[a]	23
M_2-2HPF_6-$NH_2(CH_2)_6OH$	$C_{56}H_{79}NO_{17}$	1,037.5	1,038[b]	4.8
M_2-2PF_6	$C_{62}H_{96}N_2O_{18}$	1,156.7	1,156[b]	100
M_2-2PF_6+H	$C_{62}H_{97}N_2O_{18}$	1,157.7	1,157.7[a]	100
M_2-HPF_6-$H(CH_2)_3OH$	$C_{59}H_{87}N_2O_{17}PF_6$	1,240.6	1,241.2[a]	75
M_2-HPF_6-$H(CH_2)_2OH$	$C_{60}H_{89}N_2O_{17}PF_6$	1,254.6	1,253.4[a]	65
M_2-PF_6	$C_{62}H_{96}N_2O_{18}PF_6$	1,301.6	1,302[b]	73
M_2-PF_6+Na	$C_{62}H_{96}N_2O_{18}PF_6Na$	1,324.6	1,325.9[a]	15
M_2	$C_{62}H_{96}N_2O_{18}PF_6$	1,446.6	1,447[b]	3.4
M_3-3PF_6-$NH_2(CH_2)_6OH$	$C_{87}H_{129}N_2O_{26}$	1,617.9	1,618.2[a]	9.2
M_3-3PF_6-H_2O	$C_{93}H_{142}N_3O_{26}$	1,717.0	1,717.4[a]	2.7
M_3-2HPF_6-$(CH_2)_3OH$-$(CH_2)_2OH$+Na	$C_{88}H_{130}N_3O_{25}PF_6Na$	1,797.0	1,796[b]	1.2
M_3-2PF_6-$(CH_2)_3OH$-$(CH_2)_2OH$+Na	$C_{88}H_{132}N_3O_{25}PF_6Na$	1,799.0	1,798.9[a]	8.3
M_3-HPF_6	$C_{93}H_{144}N_3O_{27}P_2F_{12}$	2,023.9	2,024[b]	1.1
M_4-PF_6	$C_{124}H_{192}N_4O_{36}P_3F_{18}$	2,748.2	2,749[b]	0.9
M_4-3PF_6-$(CH_2)_3OH$-$(CH_2)_2OH$+Na	$C_{119}H_{180}N_4O_{34}PF_6Na$	2,377.2	2,377.0[a]	3.3
M_4-3PF_6-H_2O	$C_{124}H_{190}N_4O_{35}PF_6$	2,440.3	2,440.0[a]	2.5
M_4-2PF_6-$(CH_2)_3OH$-$(CH_2)_2OH$+Na	$C_{119}H_{180}N_4O_{34}P_2F_{12}Na$	2,522.2	2,521.8[a]	15
M_5-2PF_6-2HPF_6-3OH	$C_{155}H_{235}N_5O_{42}PF_6$	2,983.6	2,983.4[a]	0.75

[a] MALDI-TOF mass spectrum recorded in the positive ion mode in dihydroxybenzoic acid matrix; sample prepared by evaporation of a chloroform/acetone (1/1 v/v) solution.

[b] FAB mass spectrum recorded in positive ion mode in nitrobenzyl alcohol; sample prepared by evaporation of a chloroform/acetone (1/1 v/v) solution.

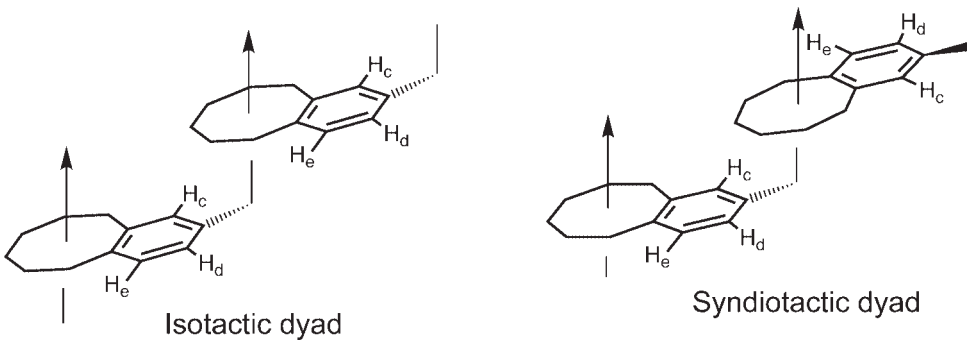

SCHEME 4 Representations of the *isotactic* and *syndiotactic* dyads resulting from self-assembly of **4** into a supramolecular polymer.

X-Ray analysis of single crystals prepared by vapor diffusion of hexane into a 1:1 solution of **9a** and DB24C8 in chloroform (10 mM each) afforded the solid state structure of the pseudorotaxane (Fig. 5). Both NH_2^+ hydrogen atoms participate in H-bonds, one with an ethyleneoxy oxygen atom (a) and one with a phenolic oxygen atom (b) of DB24C8. One of the NCH protons also is primarily hydrogen bonded to an ethyleneoxy oxygen atom (c). A somewhat unusual feature of this complex is the interaction of one of the methyl groups with one of the benzo rings of the host; one methyl proton is close to a phenolate oxygen atom of the host: CH—O distance 2.715 Å (d); this proton is also close to the benzo carbon atom, 2.714 Å (e), suggestive of a C—H—π interaction.[17] There is additional stabilization by π-stacking interaction between one of the catechol units of DB24C8 and a phenyl ring of **9a** (f). Overall the structure and packing of this pseudorotaxane are very similar to those of other dibenzylammonium salts with DB24C8[18] and derivatives.[16]

The size of the terminal aryl groups of **9b** was increased relative to that of **9a** by attaching two methoxy groups on one end and one on the other. According to CPK models, total insertion of **9b** into DB24C8 is nearly impossible even from the end with one methoxy substituent. Indeed, a single crystal structure of DB24C8 showed a cavity size of 10.2 × 4.2 Å[19] and a new polymorph isolated in this work possessed a cavity 10.4 × 2.6 Å (Fig. 6); the longer dimension is from one benzo carbon to the diagonally opposed benzo carbon and the shorter dimension refers to the closest H—H transannular distance. The energy minimized structure[20] of the trimethoxy guest **9b** has diameters of about 7.2 (methoxyphenyl end) and 9.4 Å (dimethoxyphenyl end), respectively. The bulky ends of **9b** thus seemed large enough to act as stoppers for the formation of rotaxanes from DB24C8.

In the event, the ^{1}H NMR spectrum of an equimolar (20 mM) solution of **9b** and DB24C8 in $CDCl_3$ recorded 5 min after mixing showed no sign of pseudorotaxane formation; therefore, the solution was warmed to 53 °C to provide the thermal energy required for the formation of the rotaxane by the slippage method.[1,13] Equilibrium was established after 11 days at 8% complexation, as estimated by ^{1}H NMR;[8] using the NCH_2 signals (slow exchange, analyzed as outlined above) $K_{aexp} = 5\ M^{-1}$. For synthesis of the rotaxane high temperature and high concentration will speed the formation process, although the equilibrium constant for its formation will be reduced. **9b** and DB24C8 were mixed in the solid state and heated at 150 °C (melt) for 30 min under argon. As expected, the ^{1}H NMR spectrum of the yellow chloroform solution of the heated mixture clearly displayed the peak (4.7 ppm) corresponding to the complexed benzylic protons. In contrast, the ^{1}H NMR spectrum of a nearly colorless equimolar solution of unheated **9b** and DB24C8 in $CDCl_3$ recorded one hour after mixing at room temperature showed no sign of rotaxane formation. The yellow color in the complexed solution is presumed to arise from π-stacking of the electron rich methoxyphenyl or dimethoxyphenyl ring of the guest with a relatively electron poor benzo ring of the host, assuming a coconformation of the two species similar to that of DB24C8:**9a** shown in Figure 5(e). Moreover, mass spectrometry (ESI) confirmed the formation of the rotaxane in the heated mixture (Fig. 7); the signal at *m/z* 736.3713 corresponds to $[M - PF_6]^+$ (M = DB24C8:**9b**; calculated 736.3696, error 2.3 ppm); the former signal is 0.79 times as intense as the signal at *m/z* 467.2315 for $[DB24C8 + H_3O]^+$. In contrast the solution of the unheated host and guest after standing at room temperature for 1 day revealed the rotaxane signal to the extent of only 11% of that for $[DB24C8 + H_3O]^+$; in other words, the concentration of the rotaxane

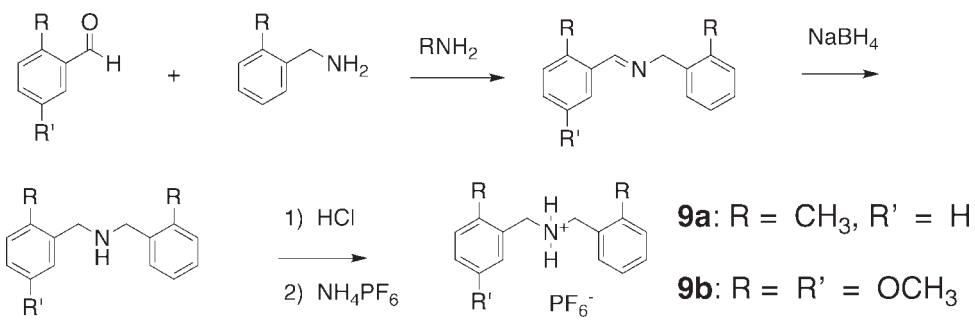

SCHEME 5 Synthesis of substituted dibenzylammonium hexafluorophosphates **9a** and **9b**.

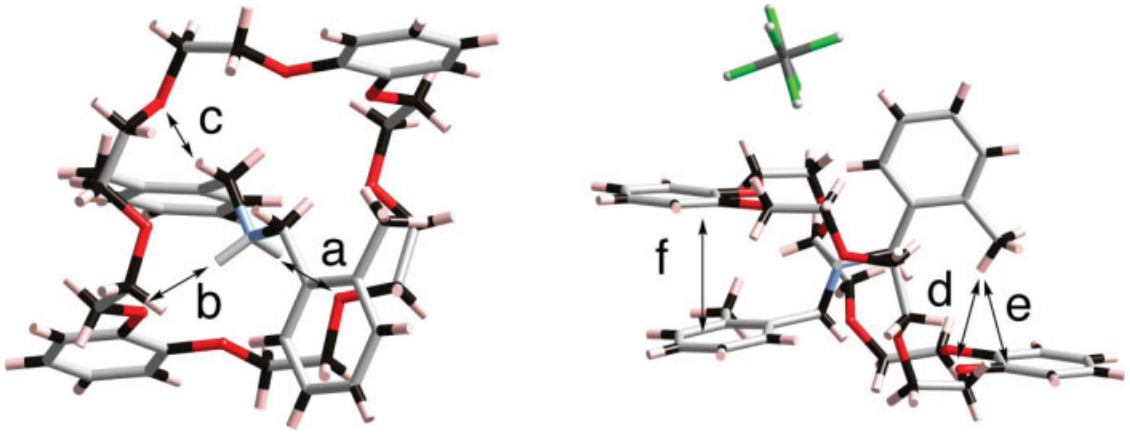

FIGURE 5 Two views of stick representations of the pseudorotaxane complex formed from **9a** and DB24C8 from X-ray crystallography; carbons are shown in black, oxygens in red, nitrogen in blue, hydrogens in pink, phosphorous in gray, and fluorines in green. Interatomic distances and angles for H-bonding: N—O (ethyleneoxy) 2.996 Å, NH(1)—O (ethyleneoxy) 2.026 Å (a), N—H—O 168.7°; N—O (phenoxy) 3.026, NH(2)—O (phenoxy) 2.060 Å (b), N—H—O 175.4°; C—O (ethyleneoxy) 3.504 Å, CH—O (ethyleneoxy) 2.582 Å (c), C—H—O 156.9°. One of tolyl groups lies at an angle of 83.35° from one of the benzo rings and its methyl carbon atoms sits 3.46 Å above that benzo ring; one of the methyl protons is 2.715 Å from the phenolic oxygen atom (d), C—H—O 148.6° and 2.714 Å from the adjacent benzo carbon (e), C—H—C 133.7°, implying some C—H—π interaction perhaps. The other tolyl ring is nearly parallel (8.39° out) to the other benzo ring and they are separated by $<$4 Å (f), indicating a π-stacking interaction.

was eightfold higher in the heated sample. The latter experiment demonstrates that threading does occur at room temperature, but relatively slowly. Attempts to isolate single crystals of this rotaxane failed.

Addition of DMSO to the chloroform solution of the heated mixture did not result in immediate dethreading as would be the case for a pseudorotaxane, since DMSO is a highly competitive hydrogen bond acceptor that essentially prevents pseudorotaxane formation.[5(d)] This clearly demonstrates that the complex is a rotaxane. The $CDCl_3$:DMSO-d_6 (1:1 v:v) solution was examined over time; the signal for the complexed benzylic protons of **9b** (4.7 ppm) persisted for several days, but was reduced in intensity relative to the signal for the uncomplexed benzylic protons and that of the α-protons of the host at 4.05 ppm.[8] The color also became less intense. The half-life was calculated to be 66 $\pm$ 10 h at room temperature in the $CDCl_3$:DMSO-d_6 (1:1 v:v) solution.

From these results, we conclude that the methoxy substituents of **9b** may be adequate for controlled slippage-type synthesis of rotaxanes based on DB24C8, although they reduce the acidity of the compound, which in turn lowers its affinity for complexation.[18]

EXPERIMENTAL

Solvents were used as received. Melting points are uncorrected. The 400 MHz ^{1}H NMR spectra were recorded on a Varian Unity instrument with tetramethylsilane (TMS) as an internal standard. The following abbreviations are used to denote splitting patterns: s (singlet), d (doublet), t (triplet), and m (multiplet). Elemental analyses were obtained from Atlantic Microlab, Norcross, GA. With the exception of Figure 7, mass spectra were provided by the Washington University Mass Spectrometry Resource. The mass spectrum of DB24C8:**9b** (Fig. 7) was obtained using an Agilent LC-ESI-TOF system.

X-Ray Crystallography

X-Ray diffraction data on complex **9a**:DB24C8 were collected on a Siemens P4/CCD diffractometer (T = 218(2) K, MoKα

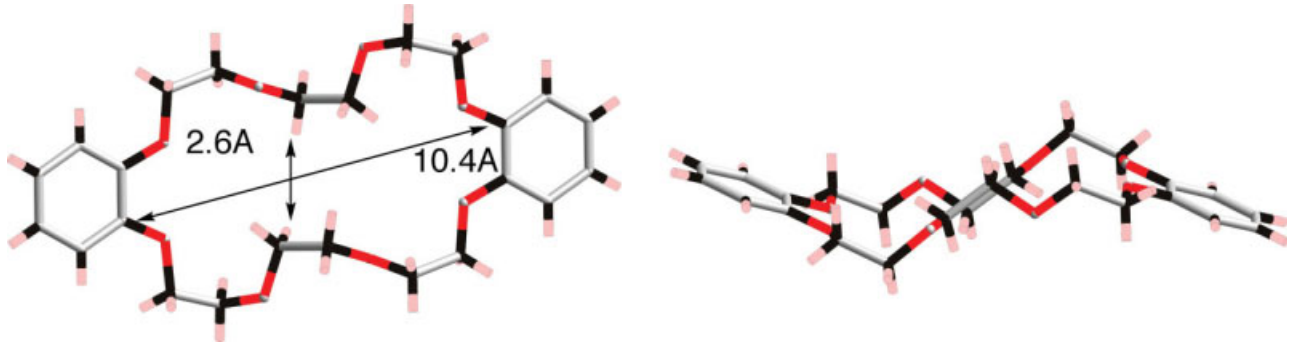

FIGURE 6 Single crystal X-ray structure of a new polymorph of dibenzo-24-crown-8: left, top view; right, side view; carbons are shown in black, oxygens in red, and hydrogens in pink.

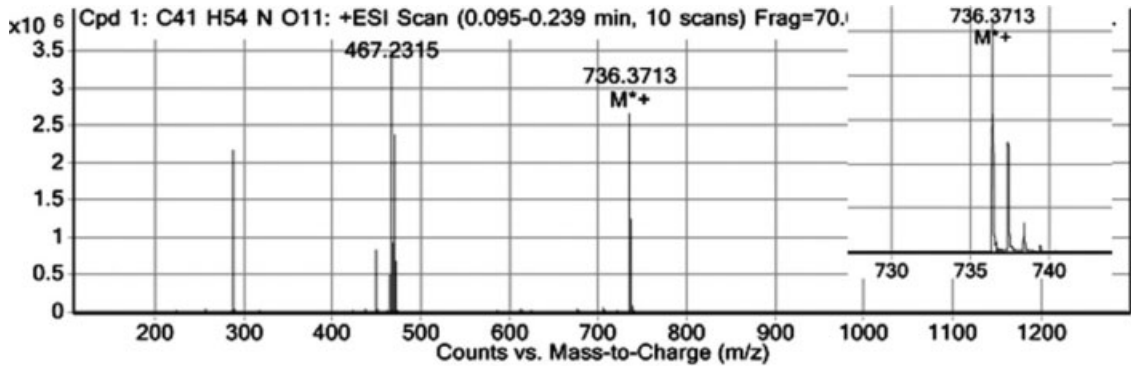

FIGURE 7 High-resolution electrospray ionization mass spectrum of an equimolar mixture of DB24C8 and trimethoxy guest **9b** heated 30 min at 150 °C under argon and then dissolved in methanol. The signal at *m/z* 736.3713 corresponds to $[M - PF_6]^+$ (calculated *m/z* 736.3691), that at *m/z* 467.2315 corresponds to $[DB24C8 + H_3O]^+$, that at *m/z* 449 corresponds to $[DB24C8 + H]^+$, and that at *m/z* 288 corresponds to guest $[\mathbf{9b}]^+$. The inset shows the isotopic M + 1, M + 2, and M + 3 peaks at *m/z* 737.3725 (47%), 738.3754 (13%), and 739 (3%).

radiation, $\theta_{max} = 23°$, 6080 independent reflections [$R_{int} = 0.0317$]). Crystal data: $C_{24}H_{32}O_8 \cdot C_{16}H_{20}NPF_6 \cdot 0.5(CHCl_3)$, FW 879.48, monoclinic, space group $P2_1/n$, $a = 10.4640(1)$ Å, $b = 11.6037(2)$ Å, $c = 35.1819(3)$ Å, $\beta = 94.927(1)°$. $V = 4256.04(7)$ Å^3, $Z = 4$, $D_c = 1.373$ g/cm^3, $\mu = 0.24$ cm^{-1}. The structure was solved by direct methods. In the crystal structure, there is an inversion disordered solvate $CHCl_3$ molecule, which was treated by the program SQUEEZE.[21] Correction of the X-ray data by SQUEEZE (119 electrons/cell) is very close to the required value (116 electrons/cell) for a demisolvate $CHCl_3$ molecule. The structure was refined with anisotropic thermal parameters for all nonhydrogen atoms. The positions of the H atoms involved in hydrogen bonding were found in the F-map and refined with isotropic thermal parameters. The positions of other H atoms were calculated. One of the O atoms (O6) in the macrocycle is disordered over two positions in ratio 82/18. Convergence was achieved with $R_1 = 0.0531$, $wR_2 = 0.1386$ and maximum residual density +0.552; −0.285 e·Å^{-3}. All software and source scattering factors are contained in the SHELXTL (5.10) program package (G. Sheldrick, Bruker XRD, Madison, WI).

Colorless needles of DB24C8 crystallized from acetone through vapor diffusion of pentane. The chosen crystal (0.06 × 0.08 × 0.40 mm^3) was centered on the goniometer of an Oxford Diffraction Gemini A Ultra diffractometer operating with MoKα radiation. The data collection routine, unit cell refinement, and data processing were carried out with the program CrysAlisPro (CrysAlisPro 171.33.34, Oxford Diffraction: Wroclaw, Poland, 2009). The Laue symmetry and systematic absences were consistent with the monoclinic space group $P2_1/n$. The structure was solved by direct methods and refined using SHELXTL NT.[22] The asymmetric unit of the structure comprises 0.5 crystallographically independent molecules. The final refinement model involved anisotropic displacement parameters for nonhydrogen atoms and a riding model for all hydrogen atoms.

2-Formyldibenzo-24-crown-8 (5)

To a stirred mixture of 0.94 g (4.4 mmol) of pyridinium chlorochromate and 40 mL dry CH_2Cl_2 was added a solution of 1.73 g (3.62 mmol) of 4-hydroxymethyldibenzo-24-crown-8[5(c)] in 10 mL of CH_2Cl_2 and stirring was continued for 2 h. The solvent was removed in vacuo and the brown residual solid was purified by recrystallization from ethanol: a white solid, 1.32 g (77%), mp 97–99 °C (lit. 5(d), 105–107 °C).

^{1}H NMR (400 MHz, $CDCl_3$, 22 °C): $\delta = 3.85$ (8H, m), 3.93 (8H, m), 4.15 (4H, m), 4.22 (4H, m), 6.88–7.44 (7H, m), and 8.92 (1H, s). Anal. calcd. for $C_{25}H_{32}O_9$: C 63.01, H 6.77; found: C 62.93, H 6.76.

General Procedure for Schiff Bases

In a 100 mL round bottom flask equipped with a Dean-Stark trap, condenser and nitrogen bubbler a solution of 12.5 mmol of aldehyde and 12.5 mmol of amine in toluene (25 mL) was refluxed for 24 h. The solvent was rotary evaporated to give the crude product, which, if a solid, was recrystallized, or used without purification to make the corresponding amine.

General Procedure for Reduction of Schiff Bases to Amines

To a 50 mL round bottom flask equipped with a magnetic stirrer were added 6.14 mmol of Schiff base and CH_3OH (25 mL). $NaBH_4$ (0.465 g, 12.3 mmol) was added slowly in small portions to the methanol solution, which was then refluxed for 12 h. The solvent was removed in vacuo to give a white solid which was suspended in H_2O and extracted with $CHCl_3$ twice. The organic layers were combined, dried over $MgSO_4$ and concentrated to afford a clear liquid, used without purification to prepare the hexafluorophosphate salt.

General Procedure for Hexafluorophosphate Salts of Secondary Amines

To a 100 mL round bottom flask equipped with a magnetic stirrer were added 2.5 mmol of amine and 2 M HCl (25 mL). The mixture was stirred for 30 min and the white precipitate

was filtered and washed with cold H_2O. This solid was dissolved in hot water and the solution was cooled to 0 °C. To this was added an aqueous solution of NH_4PF_6 until no further precipitation was observed. The precipitate was filtered and recrystallized from H_2O.

2-(Benzylideneaminomethyl)dibenzo-24-crown-8 (6a)
Recrystallized from dry ethanol, an off-white solid, mp 78–79 °C. ^{1}H NMR (400 MHz, $CDCl_3$, 22 °C): δ = 3.83 (8H, m), 3.92 (8H, m), 4.15–4.19 (8H, m), 4.79 (2H, s), 6.85–7.44 (12H, m), and 8.27 (1H, s). LR ESI MS: m/z = 588 $[M + Na]^+$. HR MALDI-TOF MS: calcd for $[M + H]^+$ $C_{32}H_{40}O_8N$: m/z = 566.2754; found: m/z = 566.2746.

2-(N-Benzylaminomethyl)dibenzo-24-crown-8 (7a)
Clear liquid, 82%. ^{1}H NMR (400 MHz, $CDCl_3$, 22 °C): δ = 3.72 (2H, s), 3.78 (2H, s), 3.83 (8H, m), 3.92 (8H, m), 4.15 (8H, m), and 6.82–7.33 (12H, m).

2-(N-Benzylammoniomethyl)dibenzo-24-crown-8 Hexafluorophosphate (4)
An off-white solid, 40%, mp 222–225 °C (lit. 5(d)) mp decomp. >210 °C). ^{1}H NMR (400 MHz, DMSO-d_6, 22 °C): δ = 3.32 (8H, m), 3.65 (8H, m), 3.75–3.79 (4H, m), 4.03–4.08 (4H, m and 2H, s), 4.12 (2H, s), 6.85–7.45 (12H, m), and 9.04 (2H, s). LR ESI MS (CH_3OH:H_2O:CH_3COOH, 59:49:1): m/z = 461.3, $[M - PF_6 - C_6H_5CH_2NH_2]^+$, 18%; 568.3, $[M - PF_6]^+$, 54%; 581.2, $[M - PF_6 + Na]^+$, base peak. HR ESI MS (CH_3OH:H_2O:CH_3COOH, 59:49:1): calcd. for $C_{32}H_{42}NO_8$ $[M - PF_6]^+$: m/z = 568.2911; $[M + 1 - PF_6]$, 36%; $[M + 2 - PF_6]$, 8%; found: m/z = 568.2904, $[M + 1 - PF_6]$, 38%; $[M + 2 - PF_6]$, 5%. HR MALDI MS: calcd for $[M - HPF_6 + Na]^+$ $C_{32}H_{41}O_8NNa$: m/z = 590.2730; found: m/z = 590.2738.

2-(6′-Hydroxyhexylideneaminomethyl)dibenzo-24-crown-8 (6b)
84%, colorless solid from toluene-hexane, mp 63–65 °C. ^{1}H NMR (400 MHz, $CDCl_3$, 22 °C): δ = 1.2–1.8 (8H, m), 3.60 (2H, t, J = 7), 3.64 (2H, t, J = 7), 3.83 (8H, m), 3.92 (8H, bs), 4.16 (6H, m), 4.22 (2H, t, J = 4), 6.8–6.9 (6H, m), 7.12 (1H, d, J = 8), 7.39 (1H, s), and 8.13 (1H, s). Anal. calcd. for $C_{31}H_{45}NO_9$: C 62.71, H 7.98, N 2.54; found: C 62.55, H 7.74, N 2.40.

2-[N-(6′-Hydroxyhexyl)aminomethyl]dibenzo-24-crown-8 (7b)
97%, very viscous oil. ^{1}H NMR (400 MHz, $CDCl_3$, 22 °C): δ = 1.35 (4H, m), 1.53 (4H, m), 2.60 (2H, t, J = 7), 3.62 (2H, t, J = 7), 3.69 (2H, s), 3.91 (8H, m), 4.15 (8H, m), 6.80 (2H, s), and 6.9 (5H, m). LR FAB MS [3-nitrobenzyl alcohol (3-NBA)/LiI]: m/z = 160.1, $[3\text{-NBA} + Li]^+$, 100%; 313.1, $[(3\text{-NBA})_2 + Li]^+$, 48%; 584.3, $[M + Li]^+$, 32%; 710.4, $[M + Cs]^+$, 8%. HR FAB MS (3-NBA/LiI): calcd. for $C_{31}H_{47}NO_9Li$: m/z = 584.3411; found: m/z = 584.3394.

2-[N-(6′-Hydroxyhexylammonio)methyl]dibenzo-24-crown-8 Hexafluorophosphate (8)
77%, colorless solid from H_2O, mp 172–173 °C. ^{1}H NMR (400 MHz, CD_3SOCD_3, 22 °C): δ = 1.27 (4H, m), 1.39 (2H, m), 1.57 (2H, m), 2.84 (2H, bs), 3.65 (8H, m), 3.75 (8H, m), 4.05 (10H, m), 4.38 (1H, t, J = 5), 6.82–7.02 (6H, m), 7.08 (1H, s), and 8.53 (2H, bs). ^{1}H NMR (400 MHz, CD_3SOCD_3, 22 °C).[8] LR FAB MS (3-NBA): see Table 1. LR FAB MS (3-NBA/LiI): m/z = 160.1, $[3\text{-NBA} + Li]^+$, 100%; 313.1, $[(3\text{-NBA})_2 + Li]^+$, 50%; 584.3, $[M - HPF_6 + Li]^+$, 38%; 710.4, $[M + Cs]^+$, 5%; 1155.4, $[M - PF_6 - HPF_6]^+$, 1%. HR FAB MS (3-NBA)/LiI): calcd. for $C_{31}H_{47}NO_9Li$: m/z = 584.3411; found: m/z = 584.3401.

o-(2-Methylbenzylideneaminomethyl)toluene
Slightly yellow liquid, bp 112–114 °C @ 0.08 Torr, 81%. ^{1}H NMR (400 MHz, $CDCl_3$, 22 °C): δ = 2.39 (3H, s), 2.50 (3H, s), 4.83 (2H, s), 7.17–7.32 (7H, m), 9.73 (1H, d, J = 7.2 Hz), and 8.67 (1H, s).

Bis(2-methylbenzyl)amine
Clear liquid, 99%. ^{1}H NMR (400 MHz, $CDCl_3$, 22 °C): δ = 2.34 (6H, s), 3.83 (4H, s), 7.16 (6H, m), and 7.33 (2H, m).

Bis(2-methylbenzyl)ammonium Hexafluorophosphate (9a)
White solid, 92%, mp 178–180 °C. ^{1}H NMR (400 MHz, $CDCl_3$, 22 °C): δ = 2.22 (6H, s), 4.25 (4H, s), 6.61 (2H, s), and 7.24–7.37 (8H, m). LR ESI MS: m/z = 226 $[M - PF_6]^+$; HR MALDI-TOF MS: calcd for $[M - PF_6]^+$ $C_{16}H_{20}N$: m/z = 226.1596; found: m/z = 226.1588.

o-(2,5-Dimethoxybenzylideneaminomethyl)anisole
Yellow liquid, 96%. ^{1}H NMR (400 MHz, $CDCl_3$, 22 °C): δ = 3.80 (3H, s), 3.83 (3H, s), 3.85 (3H, s) 4.83 (2H, s), 6.85–7.31 (6H, m), 7.58 (1H, d, J = 3.2 Hz), and 8.81 (1H, s).

o-(2,5-Dimethoxybenzylaminomethyl)anisole
Yellow liquid, 92%. ^{1}H NMR (400 MHz, $CDCl_3$, 22 °C): δ = 3.77 (6H, s), 3.80 (3H, s), 3.82 (4H, s), and 6.72–7.29 (7H, m).

o-(2,5-Dimethoxybenzylammoniomethyl)anisole Hexafluorophosphate (9b)
Yellow crystals, 94%, mp 145–147 °C. ^{1}H NMR (400 MHz, $CDCl_3$, 22 °C): δ = 3.74 (3H, s), 3.86 (3H, s), 3.90 (3H, s) 4.16 (2H, s), 4.20 (2H, s), and 6.79–7.41 (7H, m). LR ESI MS: m/z = 288 $[M\text{-}PF_6]^+$. HR MALDI-TOF MS: calcd. for $[M\text{-}PF_6]^+$ $C_{17}H_{22}N$: m/z = 288.1600; found: m/z = 288.1612.

Slippage Route to the Rotaxane from Dibenzo-24-crown-8 and Guest 9b
The host (24 mg, 54 mmol) and the guest (23.9 mg, 55 mmol) in a 10 mL pear-shaped flask were heated at 150 ± 5 °C in an oil-bath for 30 min with argon protection. The resultant yellow mixture was cooled to room temperature under argon. A portion of this solid was dissolved in $CDCl_3$ for NMR analysis.

The authors are grateful to the National Science Foundation for support of this work through grants CHE-95-21,738 and DMR-07-04,076. They also thank the Washington University Mass Spectrometry Resource, an NIH Research Resource (Grant No. P41RR0954). Furthermore, they acknowledge the National Science Foundation's support for purchase of the X-ray diffractometer (CHE-0131128) and the ESI mass spectrometer (CHE-0722638) at Virginia Tech.

REFERENCES AND NOTES

1 For reviews of pseudorotaxanes and rotaxanes see: (a) Molecular Catenanes, Rotaxanes and Knots; Sauvage, J.-P.; Dietrich-Buchecker, C. O., Eds.; Wiley-VCH: Weinheim, 1999; (b) Hubin, T. J.; Busch, D. H. Coord Chem Rev 2000, 200–202, 5–52; (c) Takata, T.; Kihara, N. Rev Heteroatom Chem 2000, 22, 197–218; (d) Huang, F.; Gibson, H. W. Prog Polym Sci 2005, 30, 982–1018; (e) Wenz, G.; Han, B.-H.; Mueller, A. Chem Rev 2006, 106, 782–817; (f) Faiz, J. A.; Heitz, V.; Sauvage, J.-P. Chem Soc Rev 2009, 38, 422–442; (g) Crowley, J. D.; Goldup, S. M.; Lee, A.-L.; Leigh, D. A.; McBurney, R. T. Chem Soc Rev 2009, 38, 1530–1541; (h) Mullen, K. M.; Beer, P. D. Chem Soc Rev 2009, 38, 1701–1713; (i) Balzani, V.; Credi, A.; Venturi, M. Chem Soc Rev 2009, 38, 1542–1550; (j) Stoddart, J. F. Chem Soc Rev 2009, 38, 1802–1820.

2 (a) Vögtle, F. Supramolecular Chemistry; Wiley: New York, 1991; (b) Cram, D. J.; Cram, J. M.; Container Molecules and Their Guests; Royal Society of Chemistry: Cambridge, 1994; (c) Lehn, J.-M. Supramolecular Chemistry; VCH: New York, 1995; (d) Comprehensive Supramolecular Chemistry; Atwood, J. L.; Davies, J. E. D.; MacNicol, D. D.; Vögtle, F., Eds.; Pergamon: New York, 1996; (e) Lindoy, L. F.; Atkinson, I. M.; Self-Assembly in Supramolecular Systems; Royal Society of Chemistry: Cambridge, 2000; (g) Gale, P. A. Adv Sci 2007, 3, 105–125; (h) Acharya, S. Adv Sci Lett 2008, 1, 28–58; (i) Harada, A.; Takashima, Y.; Yamaguchi, H. Chem Soc Rev 2009, 38, 875–882; (j) Fox, J. D.; Rowan, S. J. Macromolecules 2009, 42, 6823–6835; (k) Craig, S. L. Angew Chem Int Ed 2009, 8, 2645–2647; (l) Supramolecular Chemistry, 2nd ed.; Steed, J. W.; Atwood, J. L., Eds.; Wiley: West Sussex, UK, 2009.

3 (a) Yamaguchi, N.; Hamilton, L. M.; Gibson, H. W. Angew Chem Int Ed 1998, 37, 3275–3279; (b) Amabilino, D. B.; Ashton, P. R.; Belohradsky, M.; Raymo, F. M.; Stoddart, J. F. J Chem Soc Chem Commun 1999, 751–754; (c) Gibson, H. W.; Hamilton, L. M.; Yamaguchi, N. Polym Adv Tech 2000, 11, 791–797; (d) Jeppesen, J. O.; Perkins, J.; Becher, J.; Stoddart, J. F. Org Lett 2000, 2, 3547–3550; (e) Lee, J. W.; Ko, Y. H.; Park, S.-H.; Yamaguchi, K.; Kim, K. Angew Chem Int Ed 2001, 40, 746–749; (f) Osswald, F.; Vogel, E.; Safarowsky, O.; Schwanke, F.; Vögtle, F. Adv Synth Catal 2001, 343, 303–309; (g) Elizarov, A. M.; Chiu, S.-H.; Glink, P. T.; Stoddart, J. F. Org Lett 2002, 4, 679–682; (h) Gibson, H. W.; Yamaguchi, N.; Hamilton, L. M.; Jones, J. W. J Am Chem Soc 2002, 124, 4653–4665; (i) Jones, J. W.; Bryant, W. S.; Bosman, A. W.; Janssen, R. A. J.; Meijer, E. W.; Gibson, H. W. J Org Chem 2003, 68, 2385–2389; (j) Wang, W.; Kaifer, A. E. Angew Chem Int Ed 2006, 45, 7042–7046; (k) Leung, K. C.-F.; Arico, F.; Cantrill, S. J.; Stoddart, J. F. Macromolecules 2007, 40, 3951–3959; (l) Kim, S.-Y.; Ko, Y.; Lee, J. W.; Sakamoto, S.; Yamaguchi, K.; Kim, K. Chem Asian J 2007, 2, 747–754; (m) Zeng, Y.; Li, Y.; Li, M.; Yang, G.; Li, Y. J Am Chem Soc 2009, 131, 9100–9106.

4 A selection of recent publications on polypseudorotaxanes and polyrotaxanes: (a) Zhang, W.; Dichtel, W. R.; Stieg, A. Z.; Benitez, D.; Gimzewski, J. K.; Heath, J. R.; Stoddart, J. F.; Proc Natl Acad Sci USA 2008, 105, 6514–6519; (b) Frampton, M. J.; Sforazzini, G.; Brovelli, S.; Latini, G.; Townsend, E.; Williams, C. C.; Charas, A.; Zalewski, L.; Kaka, N. S.; Sirish, M.; Parrott, L. J.; Wilson, J. S.; Cacialli, F.; Anderson, H. L. Adv Funct Mater 2008, 18, 3367–3376; (c) Bria, M.; Bigot, J.; Cooke, G.; Lyskawa, J.; Rabani, G.; Rotello, V. M.; Woisel, P. Tetrahedron 2008, 65, 400–407; (d) Suzaki, Y.; Murata, S.; Osakada, K. Chem Lett 2009, 38, 356–357; (e) Ikeda, T.; Higuchi, M.; Kurth, D. G. J Am Chem Soc 2009, 131, 9158–9159; (f) Sato, T.; Takata, T. Polym J 2009, 41, 470–476; (g) Kato, K.; Inoue, K.; Kidowaki, M.; Ito, K. Macromolecules 2009, 42, 7129–7136; (h) Takashima, T.; Hinoue, K.; Kihara, N.; Hayashi, M.; Koyama, Y.; Takata, T. J Phys Conf Series 2009, 184, 012024; (i) Farcas, A.; Jarroux, N.; Ghosh, I.; Guegan, P.; Nau, W. M.; Harabagiu, V. Macromol Chem Phys 2009, 210, 1440–1449; (j) Gibson, H. W.; Farcas, A.; Jones, J. W.; Ge, Z.; Huang, F.; Vergne, M.; Hercules, D. M. J Polym Sci Polym Chem Ed 2009, 47, 3518–3543; (k) Lee, M.; Schoonover, D.; Gies, A.; Hercules, D. M.; Gibson, H. W. Macromolecules 2009, 42, 6483–6494; (l) Gibson, H. W.; Ge, Z.; Jones, J. W.; Harich, K.; Pederson, A.; Dorn, H. C. J Polym Sci Polym Chem Ed 2009, 47, 6472–6495.

5 (a) Ashton, P. R.; Baxter, I.; Cantrill, S. J.; Fyfe, M. C. T.; Glink, P. T.; Stoddart, J. F.; White, A. J. P.; Williams, D. J. Angew Chem Int Ed 1998, 37, 1294–1297; (b) Yamaguchi, N.; Nagvekar, D. S.; Gibson, H. W. Angew Chem Int Ed 1998, 37, 2361–2364; (c) Yamaguchi, N.; Gibson, H. W. Angew Chem Int Ed 1999, 38, 143–147; (d) Cantrill, S. J.; Youn, G. J.; Stoddart, J. F. J Org Chem 2001, 66, 6857–6872; (e) Gibson, H. W.; Yamaguchi, N.; Jones, J. W. J Am Chem Soc 2003, 125, 3522–3533; (f) Huang, F.; Gibson, H. W. J Am Chem Soc 2004, 126, 14738–14739; (g) Huang, F.; Gibson, H. W. Chem Commun 2005, 1695–1698; (h) Huang, F.; Nagvekar, D. S.; Gibson, H. W. Macromolecules 2007, 40, 3561–3567; (i) Wang, F.; Han, C.; He, C.; Zhou, Q.; Zhang, J.; Wang, C.; Li, N.; Huang, F. J Am Chem Soc 2008, 130, 11254–11255; (j) Clark, P. G.; Day, M. W.; Grubbs, R. H. J Am Chem Soc 2009, 131, 13631–13633.

6 Rev: (a) Brunsveld, L.; Folmer, B. J. B.; Meijer, E. W.; Sijbesma, R. P. Chem Rev 2001, 101, 4071–4098; (b) Harada, A.; Hashidzume, A.; Takashima, Y. Adv Polym Sci 2006, 201, 1–43; (c) Bouteiller, L. Adv Polym Sci 2007, 207, 79–112; (d) Wilson, A. J. Soft Matter 2007, 3, 409–425; (e) Dankers, P. Y. W.; Meijer, E. W. Bull Chem Soc Jpn 2007, 80, 2047–2073; (f) Binder, W. H.; Zirbs, R. Adv Polym Sci 2007, 207, 1–78; (g) ten Brinke, G.; Ruokolainen, J.; Ikkala, O. Adv Polym Sci 2007, 207, 113–177; (h) Ariga, K.; Hill, J. P.; Shundo, A.; Vinu, A.; Charvet, R.; Hoogenboom, R.; Fournier, D.; Schubert, U. S. Chem Commun 2008, 155–162; (i) Mckenzie, B. M.; Rowan, S. J. Mol Recog Polym 2008, 157–178; (j) Fiore, G. L.; Fraser, C. L. Macromolecules 2008, 41, 7892–7897.

7 (a) Yamaguchi, N.; Monthly Reports, Virginia Polytechnic Institute and State University, March 1996 to December 1997; (b) Yamaguchi, N. Ph.D. Dissertation, Virginia Polytechnic Institute and State University, 1999.

8 See Supporting Information.

9 Wu, J.; Leung, K. C.-F.; Benitez, D.; Han, J.-Y.; Cantrill, S. J.; Fang, L.; Stoddart, J. F. Angew Chem Int Ed 2008, 47, 7470–7474.

10 For a study of the efficacy of MALDI-TOF MS for such pseudorotaxanes: see Lehmann, E.; Salih, B.; Gomez-Lopez, M.; Diederich, F. Analyst 2000, 125, 849–854.

11 Kolchinski, A. G.; Busch, D. H.; Alcock, N. W. Chem Commun 1995, 1289–1291.

12 These spectra were recorded immediately after the solutions were made to avoid condensation of the ammonium salt

with acetone, yielding an iminium salt. See Jones, J. W.; Huang, F.; Bryant, W. S.; Gibson, H. W. Tetrahedron Lett 2004, 45, 5961–5963.

13 (a) Harrison, I. T. J Chem Soc Chem Commun 1971, 231–232; (b) Harrison, I. T. J Chem Soc Perk Trans 1974, 1, 301–304; (c) Schill, G.; Beckmann, W.; Schweickert, N.; Fritz, H. Chem Ber 1986, 119, 2647–2655; (d) Raymo, F. M.; Houk, K. N.; Stoddart, J. F. J Am Chem Soc 1998, 120, 9318–9322.

14 We have demonstrated that K_{aexp} is not a constant for complexation of DB24C8 and its derivatives with dibenzylammonium salts in nonpolar organic solvents; it can vary by more than an order of magnitude. The reason is that the guest salt is predominantly ion paired whereas the pseudorotaxane is not; hence, the overall process is $H + GX \rightarrow HG^{+} + X^{-}$. The expression for K_{aexp} does not include the concentration of X^{-}. To solve for the ionization constant of the salt and the binding constant of the cation with the host requires extensive data.

15 Jones, J. W.; Gibson, H. W. J Am Chem Soc 2003, 125, 7001–7004.

16 Gibson, H. W.; Wang, H.; Bonrad, K.; Jones, J. W.; Slebodnick, C.; Habenicht, B.; Lobue, P. Org Biomol Chem 2005, 3, 2114–2121.

17 (a) Nishio, M.; Umezawa, Y.; Takeuchi, Y. Tetrahedron 1995, 51, 8665–8701; (b) Nishio, M.; Hirota, M.; Umezawa, Y. The C-H–π Interaction. Evidence, Nature and Consequences; Wiley: New York, 1998; (c) Carver, F. J.; Hunter, C. A.; Jones, P. S.; Livingstone, D. J.; McCabe, J. F.; Seward, E. M.; Tiger, P.; Spey, S. E. Chem Eur J 2001, 7, 4854–4862; (d) Carver, F. J.; Hunter, C. A.; Livingstone, D. J.; McCabe, J. F.; Seward, E. M. Chem Eur J 2002, 8, 2847–2859; (e) Suezawa, H.; Ishihara, S.; Umezawa, Y.; Tsuboyama, S.; Nishio, M. Eur J Org Chem 2004, 4816–4822.; (f) Pederson, A. M.-P.; Vetor, R. C.; Rouser, M. A.; Huang, F.; Slebodnick, C.; Schoonover, D. V.; Gibson, H. W. J Org Chem 2008, 73, 5570–5573.

18 Ashton, P. R.; Fyfe, M. C. T.; Hickingbottom, S. K.; Stoddart, J. F.; White, A. J. P.; Williams, D. J. J Chem Soc Perkin Trans 1998, 2, 2117–2128.

19 Colquhoun, H. M.; Doughty, S. M.; Stoddart, J. F.; Slawin, A. M. Z.; Williams, D. J. J Chem Soc Perkin Trans 1986, 2, 253–257.

20 ChemBio3D Ultra 11.0, MM2 minimization routine.

21 van der Sluis, P.; Spek, A. L.; Acta Cryst A 1990, 46, 194–201.

22 Sheldrick, G. M. Acta Cryst A 2008, 64, 112–122.